Research paper

Experimental and numerical investigations of laminated veneer lumber panels

M. Chybiński[1], Ł. Polus[2]

Abstract: This paper presents a study of laminated veneer lumber panels subjected to bending. Laminated veneer lumber (LVL) is a sustainable building material manufactured by laminating 3-4-mm-thick wood veneers, using adhesives. The authors of this article studied the behaviour of type R laminated veneer lumber (LVL R), in which all veneers are glued together longitudinally – along the grain. Tensile, compressive and bending tests of LVL R were conducted. The short-term behaviour, load carrying-capacity, mode of failure and load-deflection of the LVL R panels were investigated. The authors observed failure modes at the collapse load, associated with the delamination and cracking of veneer layers in the tensile zone. What is more, two non-linear finite element models of the tested LVL R panel were developed and verified against the experimental results. In the 3D finite element model, LVL R was described as an elastic-perfectly plastic material. In the 2D finite element model, on the other hand, it was described as an orthotropic material and its failure was captured using the Hashin damage model. The comparison of the numerical and experimental analyses demonstrated that the adopted numerical models yielded the results similar to the experimental results.

Keywords: laminated veneer lumber, finite element analysis, engineered wood products, timber structures, composite structures, Hashin damage model

[1] Ph.D., Eng., Poznan University of Technology, Faculty of Civil and Transport Engineering, Piotrowo 5 Street, 60-965 Poznan, Poland, e-mail: marcin.chybinski@put.poznan.pl, ORCID: https://orcid.org/0000-0003-2539-7764
[2] M.Sc., Eng., Poznan University of Technology, Faculty of Civil and Transport Engineering, Piotrowo 5 Street, 60-965 Poznan, Poland, e-mail: lukasz.polus@put.poznan.pl, ORCID: https://orcid.org/0000-0002-1005-9239

1. Introduction

Timber has many advantageous attributes, e.g., it has a high strength-to-weight ratio, it is a fully renewable and largely recyclable material, and it can be produced in a wide range of shapes [1]. For these reasons, it has been used for the construction of buildings and bridges for many years [2–5]. The review presented in article [6] showed that wooden interior materials had a mainly positive or neutral effect on indoor environment quality, such as inducing positive feelings in occupants, inhibiting certain bacteria and moderating humidity fluctuations of indoor air. The negative impact of such materials on indoor environment quality, presented in article [6], was limited to volatile organic compounds emitted from wood. Timber elements may be subjected to static and dynamic loads [7]. One of the disadvantages of timber elements is that they are prone to cracking and their load-capacity and stiffness decrease with crack propagation [8–10].

New structures using timber are becoming widespread, e.g., timber-concrete composite structures [11–14], steel-timber composite structures [15, 16], aluminium-timber composite structures [17–19], timber-timber composite structures [20, 21] and timber-glass composite structures [22, 23].

Sawn timber is limited in quality and size and it usually has some defects, such as knots. Sometimes it has to be reinforced [24, 25]. For example, layered laminate bamboo composite plates, a natural and renewable material, can be used to reinforce pine beams [26]. Wood can be subjected to the process of plasticisation of its superficial layers with the objective to improve its quality as well as its strength and functional performance [27]. Furthermore, engineered wood products are developed to overcome the limitations of sawn timber. Bonded wood products may be manufactured in a factory under controlled conditions to reduce the number of defects [28]. Engineered wood products are produced in a variety of forms, such as glued-laminated timber, cross-laminated timber, plywood, laminated veneer lumber, fibreboards, chipboards, oriented strand boards or laminated strand lumber [29].

Glued-laminated timber is manufactured from 19-50-mm-thick timber laminates, bonded together with adhesives [29]. The structural behaviour of glued-laminated timber elements depends on the quality of the individual laminations, the quality of the glue-lines, the quality of the finger joints, and the integrity of the cross-section [30]. Mirski et al. assessed the feasibility of fabricating glued laminated timber from laminates made of pine wood after grading it mechanically in a horizontal arrangement [31, 32]. A model for calculating the withdrawal strength of axially-loaded self-tapping screws inserted in glued-laminated timber products was presented in [33]. Gečys et al.

presented an analysis of the strength and stiffness of steel rods glued in glulam [34]. Glued-in steel rods may be used for connecting glued-laminated timber elements.

Cross-laminated timber (CLT) is fabricated from timber boards connected by adhesive bonding. The boards are arranged perpendicularly to one another [29, 35]. CLT is optimised for bearing loads both in and out of plane [36]. CLT panels may have openings for doors, windows, and ducts [37]. Furthermore, prefabricated panels may be transported to the construction site and assembled relatively fast. Walls and floor systems made of CLT can be connected using metal connectors, such as self-tapping screws [38, 39]. Many investigations confirmed the good structural behaviour and seismic performance of CLT elements [40].

Laminated veneer lumber (LVL) is an engineered timber composite manufactured by laminating 3-4-mm-thick wood veneers, using adhesives [29]. It is a sustainable building material, which may be produced from many tree species [41]. LVL panels can be connected using scarf joints, finger joints, lap joints or tongue and groove joints [42]. LVL and structural elements made of this material have been the subject of several studies. The compressive strength of LVL perpendicular to its grain was investigated in the laboratory tests presented by Ido et al. [43]. The results of these tests suggest that the loading direction (flat-wise or edge-wise) affects the LVL strength property. LVL beams and frames jointed with glued metal plates were investigated by Pirvu et al. [44, 45]. The studied LVL portal frames with steel plates (540 × 270 × 4.5 mm) proved to be ductile and rigid. The withdrawal strength of screws in LVL was evaluated by Özçifçi [46] and by Celebi and Kilic [47]. Friction coefficients for LVL on steel surfaces were determined in laboratory tests by Dorn et al. [48]. Friction coefficient values ranged between 0.10 and 0.30 for a smooth steel surface. Determining the impact of veneer quality and thickness on the mechanical properties of LVL was the objective of the work presented in [49]. A number of studies investigate cylindrical LVL, as well as columns made of this material. Cylindrical LVL is a structural product composed of several layers of small width veneer wound along a steel mandrel [50, 51]. The bending strength of LVL at 20°C, 50°C, 100°C, 150°C, 200°C and 230°C was evaluated by Bednarek et al. [52]. Rise in temperature resulted in decreased LVL bending strength. Recently, the load-bearing capacity of LVL beams strengthened with: glass fibre reinforced polymer sheets, aramid fibre reinforced polymer sheets and carbon fibre reinforced polymer sheets has been studied [53–55]. The experimental data revealed an increase in the load-bearing capacity of the strengthened LVL beams relative to reference beams.

A numerical model of a softwood bent element was presented in [56]. The wood was modelled using Hill's Function. A numerical model of an LVL panel subjected to bending was presented in

[57]. The behaviour of LVL can be modelled using one of the techniques presented below. In the first method, LVL is treated as a composite material comprising a matrix with fictitious reinforcing fibres smeared in the principal directions [58]. In the second method, LVL is sub-dived into layers and the behaviour of LVL perpendicular to grain is described by introducing contact elements between the layers [59]. These two methods are very advanced.

In this paper, the authors described the behaviour of LVL R using two models. In the first one, LVL R was described as an elastic-perfectly plastic material. It was a simple model, which did not need many input parameters. It was also less accurate, as it did not take anisotropy or LVL R failure into account. In the second model, LVL R was described as an orthotropic material and its failure was captured using the Hashin damage model. This model, however, required many input parameters.

The main goals of this paper were:

- to investigate the short-term behaviour, load carrying-capacity, mode of failure, and load-deflection of LVL R panels,
- to develop non-linear 2D and 3D finite element models of the tested LVL R panel.

2. Materials and methods

2.1. Laminated veneer lumber

The panels used by the authors of this article in the tests were made of type R laminated veneer lumber (LVL R), in which all veneers are glued together longitudinally – along the grain. The mechanical properties of LVL R are presented in Table 1 [60].

Table 1. The material parameters of LVL R [60]

Material parameters	Value
Modulus of elasticity, parallel to grain, mean value $E_{0,mean}$ [MPa]	14 000
Modulus of elasticity, perpendicular to grain, edgewise, mean value $E_{c,90,edge,mean}$ [MPa]	430
Shear modulus, parallel to grain, edgewise, mean value $G_{0,edge,mean}$ [MPa]	600
Bending strength, flatwise, parallel to grain $f_{m,0,flat,k}$ [MPa]	50.0
Tension strength, parallel to grain $f_{t,0,k}$ [MPa]	36.0
Compression strength, parallel to grain $f_{c,0,k}$ [MPa]	40.0
Compression strength, perpendicular to grain, flatwise $f_{c,90,flat,k}$ [MPa]	3.6
Density (mean value) ρ_{mean} [kg/m^3]	550.0

LVL R is an engineered wood product fabricated from veneers of Scots pine (*Pinus sylvestris* L.) and Norway spruce (*Picea abies* L. H. Karst). The characteristic value of material strength is defined as the 5% fractile value in the EN 1990 standard [61]. Tensile, compressive and bending tests of LVL R were conducted to determine the mean values of material strength and to validate the non-linear finite element models of the LVL R panel.

2.2. Tensile tests of laminated veneer lumber

The tension strength of LVL R parallel to its grain was studied in tensile tests at room temperature and according to the EN 408 standard [62]. The tensile tests were carried out on seven samples (75×100×2450 mm), using a Zum Wald Gezu 600 testing machine (Zum Wald, Erlenbach, Switzerland) with an extensometer (see Fig. 1).
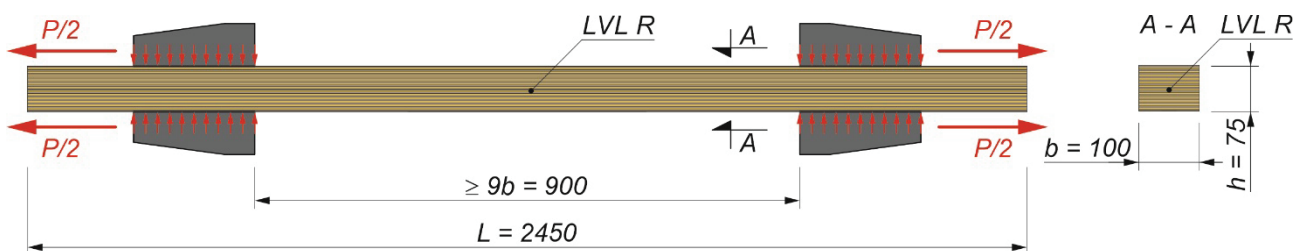
Fig. 1. The LVL R panel investigated in the tensile test

The maximum machine capacity was 600 kN. The maximum load was achieved after 300 ±120 s. In the first stage of the test, a clamping force of 3.5 N/mm^2 was applied. Next, a pre-force was applied and the stress in the sample reached 9.0 N/mm^2. After applying the pre-force, the clamping force was checked. The extensometer was used up to a point where the stress in the sample reached 28.0 N/mm^2.

2.3. Compressive tests of laminated veneer lumber

The compression strength parallel to grain was investigated in compressive tests at room temperature and according to the EN 408 standard [62]. The compressive tests were carried out using ten samples (75×200×200 mm) (see Fig. 2), and an Instron 8505 Plus testing machine (Instron, HighWycombe, Buckinghamshire, UK). The maximum machine capacity was 2000 kN. The maximum load was achieved after 300 ±120 s.
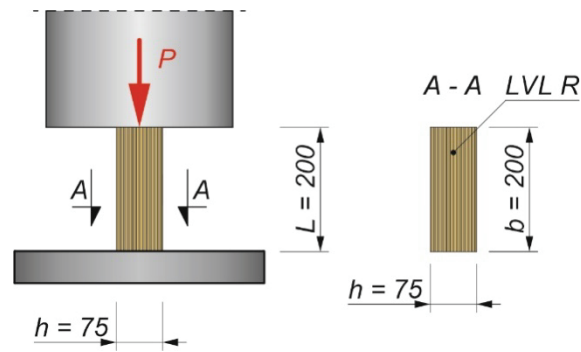
Fig. 2. The LVL R panel investigated in the compressive test

2.4. Bending tests of laminated veneer lumber

Ten LVL R panels (75×200×1950 mm) were subjected to four-point bending tests using an Instron 8505 Plus testing machine (Instron, HighWycombe, Buckinghamshire, UK) and a linear variable differential transformer (LVDT). The bending tests were conducted according to the EN 408 standard [62]. The maximum load was achieved after 300 ± 120 s. The geometric configurations and the details of such panels are presented in Fig. 3.

Fig. 3. The LVL R panel investigated in the four-point bending test

The tests were conducted in an attempt to capture the short-term local and global behaviour of LVL R panels, including the mode of failure and load-deflection response. The mid-span deflection of the LVL R panels was measured using the LVDT. The specimens were loaded symmetrically at two points of each panel, using a spreader beam (see Fig. 4). The panels were located on roller supports. Pure bending of the panels occurred between the two loading points. The piston velocity was 5.0 mm/min. Furthermore, the moisture content of the LVL R was determined using: 16 specimens, a drying chamber (Binder, Tuttlingen, Germany) and an oven dry method presented in the EN 13183-1 standard [63].
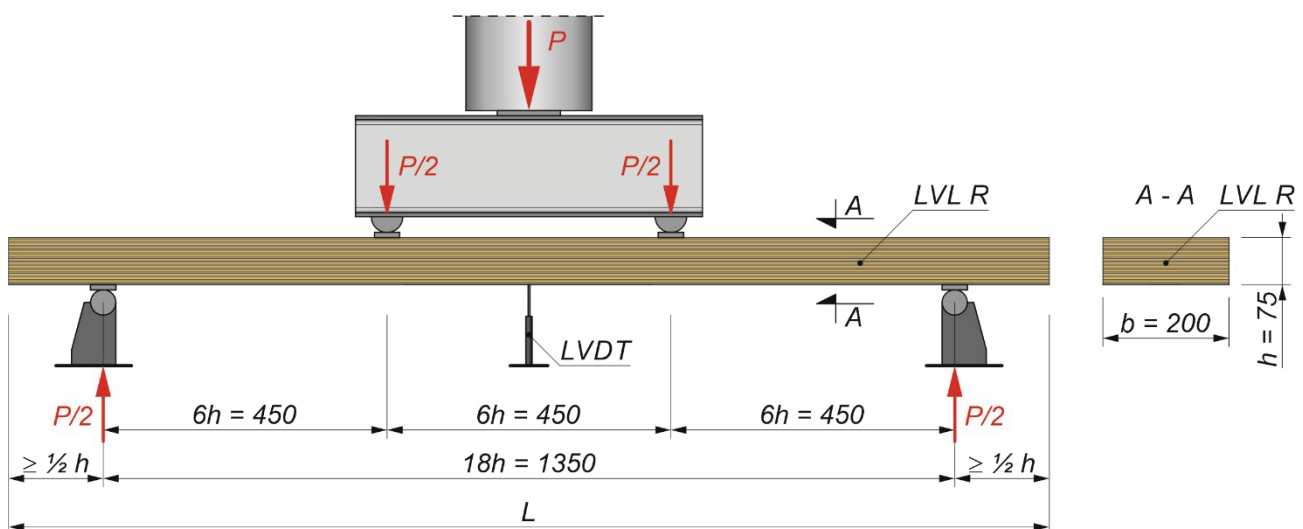
Fig. 4. Bending test set-up

3. The numerical models of the laminated veneer lumber panel

3.1. The 3D numerical model of the laminated veneer lumber panel

The 3D numerical model of the LVL R panel was prepared in the Abaqus program [64]. The authors of this article prepared only 1/4 of the model (see Fig. 5) due to fact that the panel had two axes of symmetry. The model consisted of the LVL R panel and of loading and support steel plates. The LVL R panel was divided into eight-node cuboidal finite solid elements (C3D8R) (see Fig. 6). C3D8R elements with hourglass control are often used for preparing panel and slab models. They are often used for non-linear analyses, taking into account contact, plasticity, large deformation and failure [65, 66]. Numerical analyses of structural elements described in the literature have employed C3D8R elements to model slabs, yielding accurate results when compared against laboratory test

results [67–70]. These elements should be used with reasonably fine meshes to prevent uncontrolled distortion of the mesh. In the case of a panel subjected to bending, no less than four C3D8R elements should be used through its thickness [71]. For this reason, the maximum size of the mesh was 10 mm. The steel plates were divided into linear quadrilateral elements (S4R). The total number of all elements was 7980.
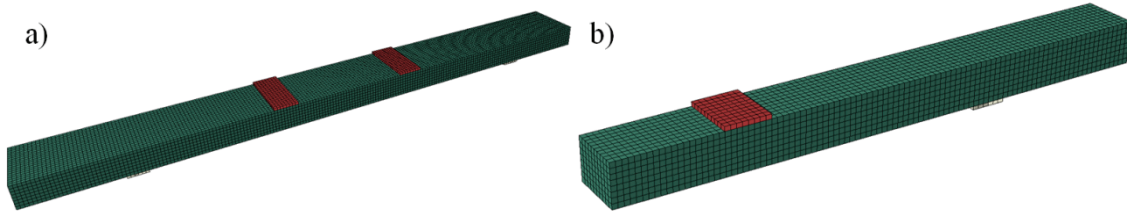
Fig. 5. The 3D model of the LVL R panel in the Abaqus program: complete panel (a), quarter of the panel (b)
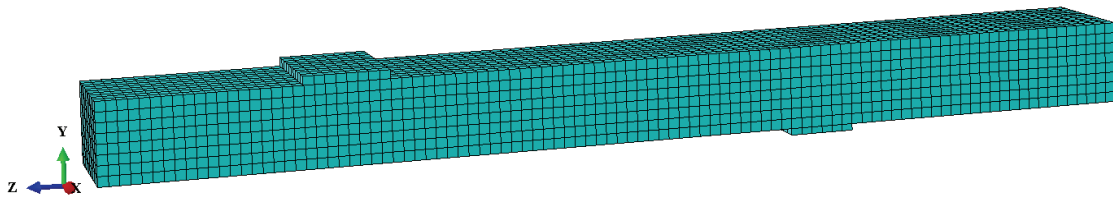
Fig. 6. The mesh used in the numerical calculations

The calculations were performed using the Newton-Raphson method. The load was applied in the form of displacement. Figure 7 presents the boundary conditions used in the computer model (fixed displacements and rotations).
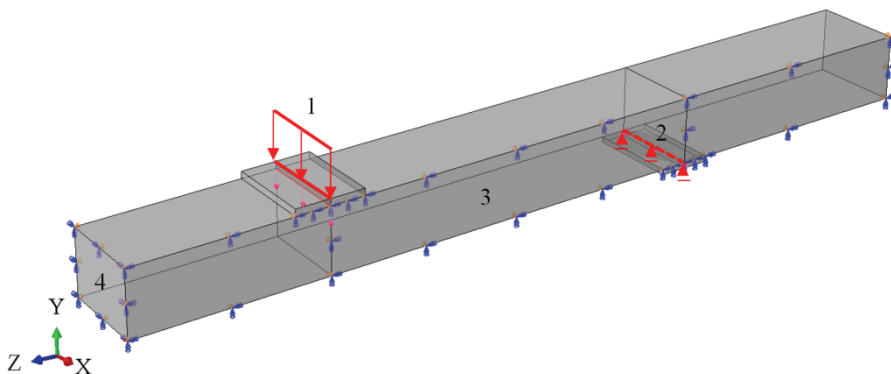
Fig. 7. Boundary conditions: 1 – displacement in y direction, 2 – displacement in y direction (fixed),
3 – displacement in x direction (fixed) and rotation around y and z axes (fixed), 4 – displacement in z direction (fixed) and rotation around x and y axes (fixed)

Friction and surface-to-surface "hard" contact were defined between the steel plates and the upper and lower surfaces of the LVL R panel. The value of the friction coefficient was equal to 0.3 based on the laboratory tests conducted by Dorn et al. [48].

The properties of LVL R adopted in the finite element model are presented in Table 2. The LVL R was modelled as an elastic-perfectly plastic material. However, this model did not take LVL R failure into account. Due to this fact, the authors made an assumption that the resistance of the LVL R panel was achieved when LVL R exceeded both the compression strength at the upper part of the LVL R panel and the tensile strength at the bottom part of the LVL R panel.

Table 2. The properties of LVL R adopted in the 3D numerical model

Material parameters	Value
Young's modulus [MPa]	14 000 [1]
Poisson's ratio [-]	0.48 [2]
Compression strength parallel to grain [MPa]	50.3 [3]
Logarithmic plastic strain [MPa]	0.0 [4]

[1] based on [60], [2] based on [16], [3] based on the compressive tests presented in this paper, [4] without strain hardening.

3.2. The 2D numerical model of the laminated veneer lumber panel

The 2D numerical model of the LVL R panel was prepared in the Abaqus program [64]. The LVL R panel and the support and loading steel plates were modelled using 4-node bilinear plane stress quadrilateral elements with reduced integration and hourglass control (CPS4R). The maximum size of the mesh was 5 mm. The total number of all elements was 5938 (see Fig. 8).
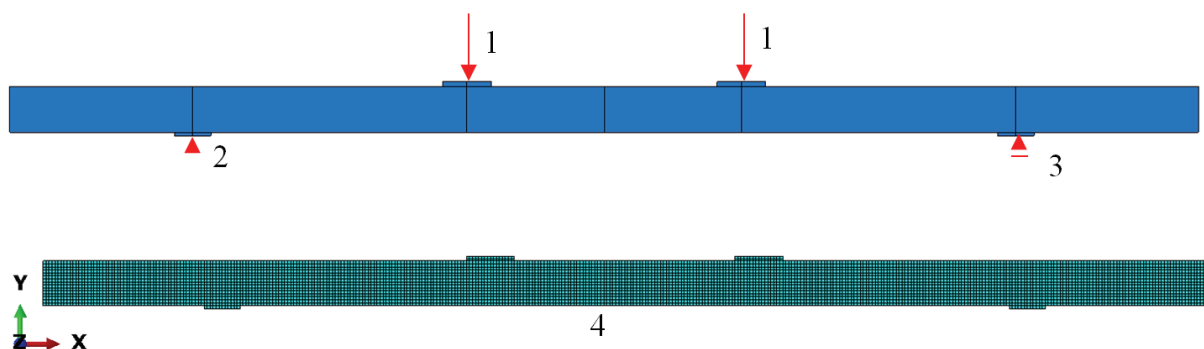
Fig. 8. The 2D model of the LVL R panel in the Abaqus program: 1 – displacement in y direction, 2 – displacement in x and y directions (fixed), 3 – displacement in y direction (fixed), 4 – mesh

Hassanieh et al. employed CPS4R elements to model an LVL slab of a composite steel-timber beam and their numerical models adequately captured the behaviour of the steel timber beams tested in laboratory conditions [16]. The calculations were performed using the Newton-Raphson method. The load was applied in the form of displacement. Figure 8 presents the boundary conditions used in the model. Friction and surface-to-surface "hard" contact were defined between the support and loading steel plates and the upper and lower surfaces of the LVL R panel. The value of the friction coefficient was equal to 0.3 based on the results presented in [48].

In the 2D FE model, steel was described as an elastic-perfectly plastic material ($E = 210\,000$ MPa, $v = 0.3$, $f_y = 235$ MPa). LVL R was described as an orthotropic material. Under plane stress conditions and for an orthotropic material, the stress-strain relations are of the form [64]:

$$(3.1) \qquad \begin{Bmatrix} \varepsilon_1 \\ \varepsilon_2 \\ \gamma_{12} \end{Bmatrix} = \begin{bmatrix} 1/E_1 & -v_{12}/E_1 & 0 \\ -v_{12}/E_1 & 1/E_2 & 0 \\ 0 & 0 & 1/G_{12} \end{bmatrix} \begin{Bmatrix} \sigma_{11} \\ \sigma_{22} \\ \tau_{12} \end{Bmatrix}$$

LVL R failure was captured using the Hashin damage model available in the material library of the Abaqus program [64]. The accuracy of this model in describing the behaviour and failure of LVL was studied by Valipour et al. [58] and Khorsandnia et al. [59]. The following variables relate to damage initiation in the Hashin damage model [64, 72, 73]:

- HSNFTCRT – the maximum value of the fibre tensile initiation criterion (damage due to the tension of the fibres),
- HSNFCCRT – the maximum value of the fibre compressive initiation criterion (damage due to the compression of the fibres),
- HSNMTCRT – the maximum value of the matrix tensile initiation criterion,
- HSNMCCRT – the maximum value of the matrix compressive initiation criterion.

The variables above indicate whether the initiation criterion in the Hashin damage mode has been satisfied or not. A value of 1.0 means that the criterion has been satisfied, while a value below 1.0 shows that the criterion has not been satisfied. The Hashin damage model cannot be used when the LVL R panels are modelled using solid 3D elements [64], e.g. in the 3D model presented in Chapter 3.1.

The material properties of the LVL R used in the numerical analyses are presented in Table 3. The parameters were found in the literature, were based on experiment results or were determined by matching the simulation and the experiment results.

Table 3. The properties of the LVL R adopted in the 2D numerical model

Properties for an elastic orthotropic material (type: lamina)					
E_1 [a] [MPa]	E_2 [MPa]	v_{12} [–]	G_{12} [MPa]	G_{13} [MPa]	G_{23} [MPa]
16 000.0 [b]	430.0 [c]	0.48 [d]	600.0 [c]	600.0 [c]	96.0 [d]
Hashin damage parameters					
Longitudinal tensile strength [MPa]	Longitudinal compressive strength [MPa]	Transverse tensile strength [MPa]	Transverse compressive strength [MPa]	Longitudinal shear strength [MPa]	Transverse shear strength [MPa]
41.9 [e]	50.3 [e]	10.0 [d]	15.0 [d]	10.0 [d]	5.0 [d]
Longitudinal tensile fracture energy [kJ/m^2]	Longitudinal compressive fracture energy [kJ/m^2]	Transverse tensile fracture energy [kJ/m^2]	Transverse compressive fracture energy [kJ/m^2]	Viscosity coefficient [–]	
45.0 [b]	45.0 [b]	0.1 [b]	0.1 [b]	1.0×10^{-6} [b]	
[a] direction 1 is parallel to the LVL R grain;					
[b] determined based on matching the simulation and the experiment results;					
[c] based on [60];					
[d] based on [16];					
[e] based on the laboratory tests presented in this paper.					

4. Results of the laboratory tests

4.1. The results of the tensile tests

The tension strength parallel to grain was 41.9 MPa ±4.8 (11.5%). The measurement errors for the tension strength of the LVL R were calculated using Student's t-distribution with 6 degrees of freedom and a confidence level of 0.95. The mode of failure was associated with the shearing of the veneer layers (see Fig. 9).

The presence of knots and butt joints might have had an impact on the configuration of the failure [67, 74]. The characteristic tension resistance from the tests (36.7 MPa) was 1.9% higher than the characteristic value of tension strength (36.0 MPa) declared by the manufacturer in [60]. The extensometer was not used throughout the entire test. For this reason, the authors did not present the curves from the laboratory tensile tests.

Fig. 9. The failure mode of the LVL R panel in the tensile test

4.2. The results of the compressive test

The compression strength parallel to grain was 50.3 MPa ±1.6 (3.2%). The measurement errors for the compression strength of the LVL R were calculated using Student's t-distribution with 9 degrees of freedom and a confidence level of 0.95. The mode of failure was associated with the cambering of the veneer layers (see Fig. 10).

Fig. 10. The failure modes of the LVL R panels in the compressive tests

The characteristic compression resistance from the tests (48.7 MPa) was 17.9% higher than the characteristic value of compression strength (40.0 MPa) declared by the manufacturer in [60]. Figure 11 shows the load versus displacement curves from the laboratory compressive tests.
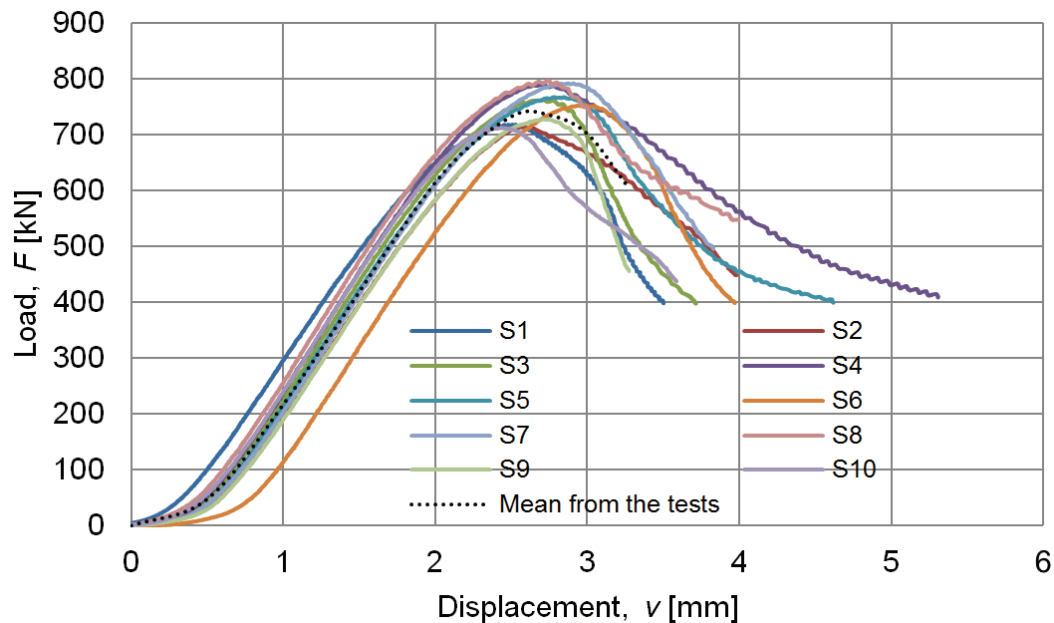
Fig. 11. The load versus displacement curves from the laboratory compressive tests

4.3. The results of the bending tests

The results of the bending tests are presented in Fig. 12 and in Table 4. Figure 12 shows the load versus mid-span deflection curves from the laboratory tests. The following symbols were used in Table 4: F_{ult} – ultimate load, M_u – ultimate load-carrying capacity of the LVL R panel, u_{ult} – mid-span deflection corresponding to M_u. The bending strength, flatwise, parallel to grain was 66.1 MPa ±6.9 MPa (10.4%). The moisture content of the LVL R was 7.9% ±0.1 (1.7%) and the density of the LVL R was 613.0 kg/m^3 ±7.1 (1.2%). The measurement errors for the bending strength and the density of the LVL R were calculated using Student's t-distribution with 7 degrees of freedom and a confidence level of 0.95. The measurement errors for the moisture content of the LVL R were calculated using Student's t-distribution with 15 degrees of freedom and a confidence level of 0.95. The characteristic bending resistance from the tests (59.2 MPa) was 15.5% higher than the characteristic value of bending strength (50.0 MPa) declared by the manufacturer in [60].
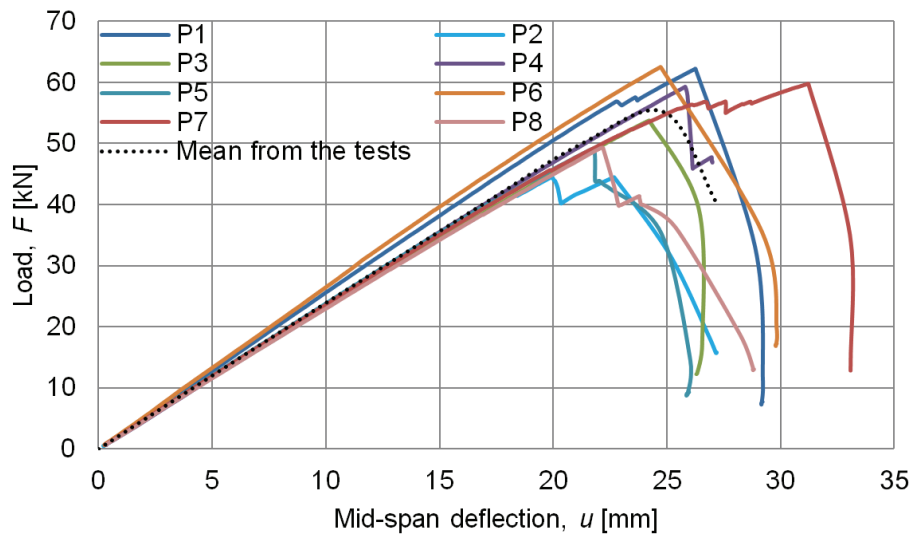
Fig. 12. The load versus mid-span deflection curves from the laboratory bending tests

Table 4. The results of the bending tests

Parameter	Mean from the tests (T)
F_{ult} [kN]	55.1 ± 5.7 (10.4%)
M_u [kN·m]	12.4 ± 1.3 (10.4%)
u_{ult} [mm]	24.9 ± 2.6 (10.3%)

The failure mechanisms which occurred in the laboratory tests manifested themselves in the local delamination and cracking of the external veneer layers in the tensioned zone of the LVL R panel (see Fig. 13). The mode of failure was associated with excessive deflection and stress at mid-span.

Fig. 13. The failure mode of the LVL R panel from the bending test

5. Results of the numerical investigations

5.1. The results of the finite element analysis of the 3D numerical model

In the finite element analysis of the 3D model, the authors of this paper assumed that the load-bearing capacity of the LVL R panel was achieved when the LVL R exceeded both the compression strength at the upper part of the LVL R panel and the tensile strength at the bottom part of the LVL R panel (see Fig. 14).
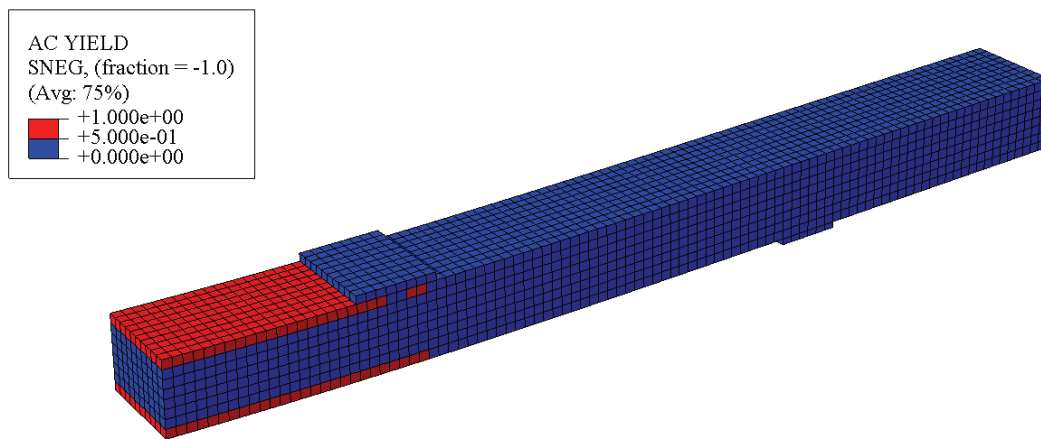
Fig. 14. The achieved load-bearing capacity of the LVL R panel (F_{ult} = 51.6 kN)

Due to the fact that the model of LVL R used in the 3D model did not distinguish between compressive and tensile strength, the authors used the mean compressive strength of the LVL R from the laboratory tests as the maximum stress which may occur in LVL R modelled in the Abaqus program.

5.2. The results of the finite element analysis of the 2D numerical model

The numerical analysis of the 2D model allowed for the assessment of damage initiation in the compressed fibres (see Fig. 15) and tensioned fibres (see Fig. 16). The failure of the LVL R panel occurred in the middle, at the upper and bottom parts of the panel, where the stress was the highest.
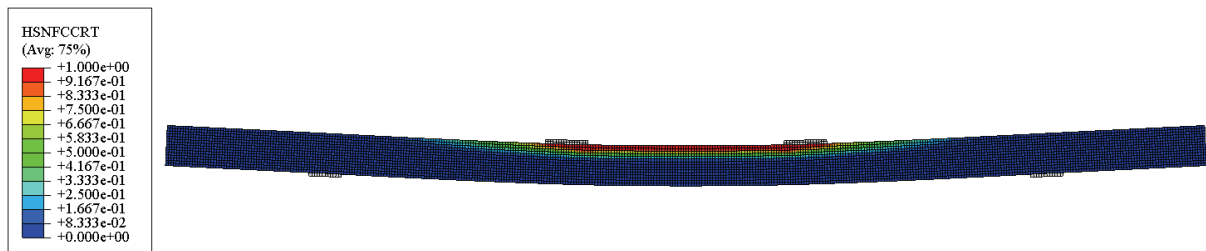
Fig. 15. Damage initiation areas due to the compression of the fibres for the ultimate load (F_{ult} = 47.4 kN)
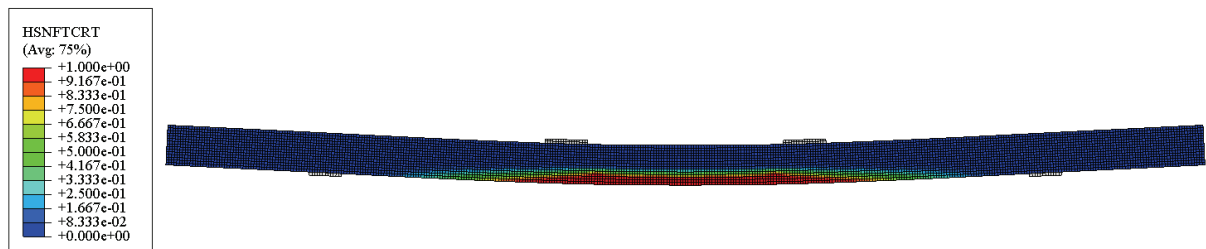
Fig. 16. Damage initiation areas due to the tension of the fibres for the ultimate load (F_{ult} = 47.4 kN)

5.3. A comparison of the results of the experimental and numerical investigations

The results of the bending tests and the numerical analyses are compared and contrasted in Table 5.

Table 5. The results of the bending tests and the finite element analyses

Parameter	Mean from the tests (T)	FEA 3D (A)	FEA 2D (B)	(T)/(A)	(T)/(B)
F_{ult} [kN]	55.1 ± 5.7 (10.4%)	51.6	47.4	1.07	1.16
M_u [kN·m]	12.4 ± 1.3 (10.4%)	11.6	10.7	1.07	1.16
u_{ult} [mm]	24.9 ± 2.6 (10.3%)	25.1	23.9	0.99	1.04

Figure 17 shows the mean load-deflection curve from the laboratory tests and the load-deflection curves from the FEA. As can be seen, the adopted models captured the response of the LVL R panel fairly well.

The ultimate load-carrying capacity from the FEA of the 3D model (11.6 kN·m) was 7% lower than the mean ultimate load-carrying capacity from the tests (12.4 kN·m). The value of the ultimate moment capacity from the numerical analysis of the 2D model (10.7 kN·m) was 16% lower than the mean moment capacity from the bending tests. The values of the ultimate load-carrying capacity from the finite element analyses were between the maximum and minimum values from the laboratory tests (see Fig. 18). There was a peak on the mean load-deflection curve from the FEA of

the 2D model, because in this model the damage of LVL R was taken into account. In the 3D model, the LVL R was modelled without taking damage into account and the calculations were terminated when the LVL R exceeded both the compression strength at the upper part of the LVL R panel and the tensile strength at the bottom part of the LVL R panel.

The numerical 2D model had higher initial stiffness than the numerical 3D model. In the 3D model, the modulus of elasticity parallel to grain for LVL R (14.0 GPa) was taken as the mean value from the manufacturer's specifications. In the 2D model, the higher value of the modulus of elasticity parallel to grain for LVL R (16.0 GPa) was used based on matching the simulation and the experiment results.
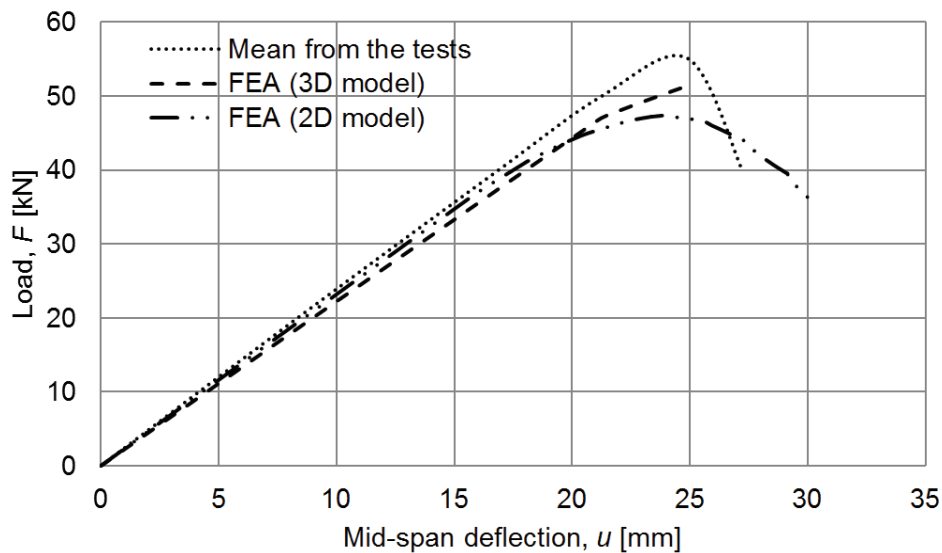
Fig. 17. The mean load-deflection curve from the laboratory tests and the load-deflection curves from the FEA
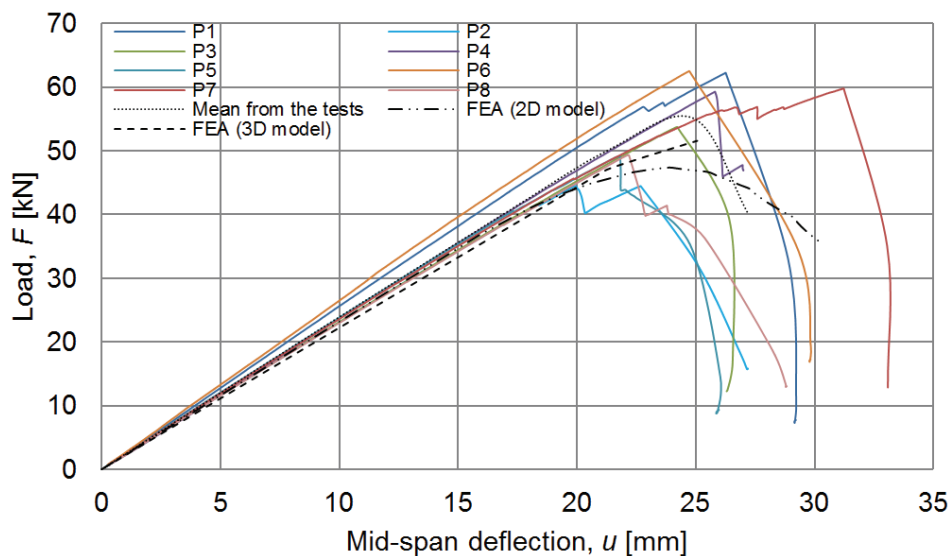
Fig. 18. The load versus mid-span deflection curves from the FEA and the laboratory tests

6. Conclusions

The authors of this article investigated the short-term structural behaviour of LVL R panels subjected to bending. They observed failure modes at the collapse load, associated with the delamination and cracking of veneer layers in the tensile zone. In addition, two finite element models of the LVL R panel were developed using the Abaqus program. In the 3D model, LVL R was described as an elastic-perfectly plastic material. However, this model did not take into account LVL R anisotropy or failure. Due to the fact that the behaviour of LVL R was captured using a simple model, it was necessary to make the assumption that the ultimate load-carrying capacity of an LVL R panel was achieved when the LVL R exceeded both the compression strength at the upper part of the LVL R panel and the tensile strength at the bottom part of the LVL R panel. In the 2D model, LVL R was described as an orthotropic material and its failure was captured using the Hashin damage model. However, this model needed many input parameters.

The discussed numerical models may be used in further numerical analyses of LVL R panels, e.g., to evaluate the impact of LVL R panel dimensions on its load-bearing capacity. Furthermore, the authors of this paper are also investigating aluminium-timber composite beams with LVL R panels [17]. The models of LVL R presented in this paper may be used to study these composite elements.

References

[1] A. M. Harte, "Timber engineering: an introduction", in *ICE Manual of Construction Materials: Volume I/II: Fundamentals and theory; Concrete; Asphalts in road construction; Masonry*, M. Forde, Ed., ICE Publishing, Chapter 60, 2009.

[2] A. Karolak, J. Jasieńko and R. Raszczuk, "Historical scarf and splice carpentry joints: state of the art", *Heritage Science*, vol. 8, article number 105, 2020. https://doi.org/10.1186/s40494-020-00448-2

[3] P. Witomski, A. Krajewski and P. Kozakiewicz, "Selected mechanical properties of Scots pine wood from antique churches of Central Poland", *European Journal of Wood and Wood Products,* vol. 72, pp. 293–296, 2014. https://doi.org/10.1007/s00107-014-0783-y

[4] E. Kotwica and S. Krzosek, "Timber bridges – revive of old and new bridges built in Switzerland", *Annals of Warsaw University of Life Sciences – SGGW, Forestry and Wood Technology*, vol. 92, pp. 207-210, 2015.

[5] B. Franke, S. Franke, A. Müller, M. Vogel, F. Scharmacher and T. Tannert, "Long term monitoring of timber bridges – Assessment and results", *Advanced Materials Research*, vol. 778, pp. 749–756, 2013. https://doi.org/10.4028/www.scientific.net/AMR.778.749

[6] T. Alapieti, R. Mikkola, P. Pasanen and H. Salonen, "The influence of wooden interior materials on indoor environment: a review", *European Journal of Wood and Wood Products*, vol. 78, pp. 617–634, 2020. https://doi.org/10.1007/s00107-020-01532-x

[7] A. Bragov, L. Igumnov, F. dell'Isola, A. Konstantinov, A. Lomunov and T. Iuzhina, "Dynamic testing of lime-tree (*Tilia Europoea*) and pine (*Pinaceae*) for wood model identification", *Materials*, vol. 13, no. 22, article 5261, 2020. https://doi.org/10.3390/ma13225261

[8] P. G. Kossakowski, "Influence of anisotropy on the energy release rate G_I for highly orthotropic materials", *Journal of Theoretical and Applied Mechanics*, vol. 45, no. 4, pp. 739–752, 2007.

[9]   P. G. Kossakowski, "Fracture toughness of pine wood for I and II loading modes", *Archives of Civil Engineering*, vol. 54, no. 3, pp. 509–529, 2008.

[10] P. G. Kossakowski, "Mixed mode I/II fracture toughness of pine wood", *Archives of Civil Engineering*, vol. 55, no. 2, pp. 199–227, 2009.

[11] M. Szumigała, E. Szumigała and Ł. Polus, "Laboratory tests of new connectors for timber-concrete composite structures", *Engineering Transactions*, vol. 66, no. 2, pp. 161–173, 2018.

[12] M. Fragiacomo and E. Łukaszewska, "Time-dependent behaviour of timber-concrete composite floors with prefabricated concrete slabs", *Engineering Structures*, vol. 52, pp. 687–696, 2013. https://doi.org/10.1016/j.engstruct.2013.03.031

[13] A. Dias, J. Skinner, K. Crews and T. Tannert, "Timber-concrete-composites increasing the use of timber in construction", *European Journal of Wood and Wood Products*, vol. 74, no. 3, pp. 443–451. 2016. https://doi.org/10.1007/s00107-015-0975-0

[14] N. Khorsandnia, H. R. Valipour and K. Crews, "Experimental and analytical investigation of short-term behavior of LVL-concrete composite connections and beams", *Construction and Building Materials*, vol. 37, pp. 229–238, 2012. https://doi.org/10.1016/j.conbuildmat.2012.07.022

[15] P. Kyvelou, L. Gardner and D. A. Nethercot, "Testing and analysis of composite cold-formed steel - wood-based flooring systems", *Journal of Structural Engineering*, vol. 143, no. 11, 2017. https://doi.org/10.1061/(ASCE)ST.1943-541X.0001885

[16] A. Hassanieh, H. R. Valipour and M. A. Bradford, "Experimental and numerical study of steel-timber composite (STC) beams", *Journal of Constructional Steel Research*, vol. 122, pp. 367–378, 2016. https://doi.org/10.1016/j.jcsr.2016.04.005

[17] M. Chybiński and Ł. Polus, "Theoretical, experimental and numerical study of aluminium-timber composite beams with screwed connections", *Construction and Building Materials*, vol. 226, pp. 317–330. 2019. https://doi.org/10.1016/j.conbuildmat.2019.07.101

[18] S. M. Saleh and N. A. Jasim, "Structural behavior of timber aluminum composite beams under static loads", *International Journal of Research in Engineering and Technology*, vol. 3, no. 10, pp. 1166–1173, 2014.

[19] M. Szumigała, M. Chybiński and Ł. Polus, "Preliminary analysis of the aluminium-timber composite beams", *Civil and Environmental Engineering Reports*, vol. 27, no. 4, pp. 131–141, 2017. https://doi.org/10.1515/ceer-2017-0056

[20] C. Bedon and M. Fragiacomo, "Numerical analysis of timber-to-timber joints and composite beams with inclined self-tapping screws", *Composite Structures*, vol. 207, pp. 13–28, 2019. https://doi.org/10.1016/j.compstruct.2018.09.008

[21] G. Schiro, I. Giongo, W. Sebastian, D. Riccadonna and M. Piazza, "Testing of timber-to-timber screw-connections in hybrid configurations", *Construction and Building Materials*, vol. 171, pp. 170–186, 2018. https://doi.org/10.1016/j.conbuildmat.2018.03.078

[22] K. Furtak and K. Rodacki, "Experimental investigations of load-bearing capacity of composite timber-glass I-beams", *Archives of Civil and Mechanical Engineering*, vol. 18, no. 3, pp. 956–964, 2018. https://doi.org/10.1016/j.acme.2018.02.002

[23] M. Kozłowski, M. Kadela and J. Hulimka, "Numerical investigation of structural behavior of timber-glass composite beams", *Procedia Engineering*, vol. 161, pp. 78–89, 2016. https://doi.org/10.1016/j.proeng.2016.08.838

[24] P. Rapp, "Application of adhesive joints in reinforcement and reconstruction of weakened wooden elements loaded axially", *Drewno*, vol. 59, no. 196, pp. 59–73, 2016. https://doi.org/10.12841/wood.1644-3985.128.05

[25] P. Rapp, "The numerical modeling of adhesive joints in reinforcement of wooden elements, subjected to bending and shearing", *Drewno*, vol. 60, no. 199, pp. 21–36, 2017. https://doi.org/10.12841/wood.1644-3985.192.02

[26] I. Burawska, M. Zbieć, A. Tomusiak and P. Beer, "Local reinforcement of timber with composite and lignocellulosic materials", *BioResources*, vol. 10, 457–468, 2015.

[27] M. Dudziak, I. Malujda, K. Talaśka, T. Łodygowski and W. Sumelka, "Analysis of the process of wood plasticization by hot rolling", *Journal of Theoretical and Applied Mechanics*, vol. 54, no. 2, pp. 503–516. 2016. https://doi.org/10.15632/jtam-pl.54.2.503

[28] M. Wieruszewski, G. Gołuński, G. J. Hruzik and V. Gotych, "Glued elements for construction", *Annals of Warsaw University of Life Sciences – SGGW Forestry and Wood Technology*, vol. 72, pp. 453–458, 2010.

[29] J. Porteous and A. Kermani, "Structural Timber Design to Eurocode 5", 2nd ed., Chichester: Wiley-Blackwell, 2013.

[30] P. Dietsch and T. Tannert, "Assessing the integrity of glued-laminated timber elements", *Construction and Building Materials*, vol. 101, no. 2, pp. 1259–1270, 2015. https://doi.org/10.1016/j.conbuildmat.2015.06.064

[31] R. Mirski, D. Dziurka, M. Chuda-Kowalska, M. Wieruszewski, J. Kawalerczyk and A. Trociński, "The usefulness of pine timber (*Pinus sylvestris* L.) for the production of structural elements. Part I: Evaluation of the quality of the pine timber in the bending test", *Materials*, vol. 13, article 3957, 2020. https://doi.org/10.3390/ma13183957

[32] R. Mirski, D. Dziurka, M. Chuda-Kowalska, J. Kawalerczyk, M. Kuliński and K. Łabęda, "The usefulness of pine timber (*Pinus sylvestris* L.) for the production of structural elements. Part II: Strength properties of glued laminated timber", *Materials*, vol. 13, article 4029, 2020. https://doi.org/10.3390/ma13184029

[33] R. Brandner, A. Ringhofer and T. Reichinger, "Performance of axially-loaded self-tapping screws in hardwood: Properties and design", *Engineering Structures*, vol. 188, pp. 677–699, 2019. https://doi.org/10.1016/j.engstruct.2019.03.018

[34] T. Gečys, G. Šaučiuvėnas, L. Ustinovichius, C. Miedzialowski and P. Sulik, "Surface based cohesive behavior implementation for the strength analysis of glued-in threaded rods in glulam", *Bulletin of the Polish Academy of Sciences Technical Sciences*, vol. 68, no. 5, pp. 1149–1157, 2020. https://doi.org/10.24425/bpasts.2020.134665

[35] R. Brandner, "Production and technology of cross laminated timber (CLT): State-of-the-art report", in *European Conference on Cross Laminated Timber*, R. Harris, A. Ringhofer and G. Schickhofer, Eds., Graz: Graz University of Technology, 2013, pp. 3–36.

[36] M. Jeleč, D. Varevac and V. Rajčić, "Cross-laminated timber (CLT) – a state of the art report", *Građevinar*, vol. 70, no. 2, pp. 75–95, 2018. https://doi.org/10.14256/JCE.2071.2017

[37] O. Espinoza, V. R. Trujillo, M. F. Laguarda and U. Buehlmann, "Cross-laminated timber: Status and research needs in Europe", *BioResources*, vol. 11, pp. 281–295, 2016.

[38] A. Ringhofer, R. Brandner and H. J. Blaß, "Cross laminated timber (CLT): Design approaches for dowel-type fasteners and connections", *Engineering Structures*, vol. 171, pp. 849–861, 2018. https://doi.org/10.1016/j.engstruct.2018.05.032

[39] R. Brandner, A. Ringhofer and M. Grabner, "Probabilistic models for the withdrawal behavior of single self-tapping screws in the narrow face of cross laminated timber (CLT)", *European Journal of Wood and Wood Products*, vol. 76, no. 1, pp. 13–30, 2018. https://doi.org/10.1007/s00107-017-1226-3

[40] T. Tannert, M. Follesa, M. Fragiacomo, P. González, H. Isoda, D. Moroder, H. Xiong and J. van de Lindt, "Seismic Design of Cross-laminated Timber Buildings", *Wood and Fiber Science*, vol. 50, pp. 3–26, 2018.

[41] Z. Chena, Q. Lei, R. He, Z. Zhang, A. Jalal Khan Chowdhury, "Review on antibacterial biocomposites of structural laminated veneer lumber", *Saudi Journal of Biological Sciences*, vol. 23, no. 1, pp. 142–147, 2016. https://doi.org/10.1016/j.sjbs.2015.09.025

[42] A. Özçifçi, "Effect of scarf joints on bending strength and modulus of elasticity to laminated veneer lumber (LVL)", *Building and Environment*, vol. 42, pp. 1510–1514, 2007. https://doi.org/10.1016/j.buildenv.2005.12.024

[43] H. Ido, H. Nagao, H. Kato, A. Miyatake and Y. Hiramatsu, "Strength properties of laminated veneer lumber in compression perpendicular to its grain", *Journal of Wood Science*, vol. 56, pp. 422–428, 2010. https://doi.org/10.1007/s10086-010-1116-3

[44] C. Pirvu, H. Yoshida and K. Taki, "Development of LVL frame structures using glued metal plate joints I: bond quality and joint performance of LVL-metal joints using epoxy resins", *Journal of Wood Science*, vol. 45, pp. 284–290, 1999. https://doi.org/10.1007/BF00833492

[45] C. Pirvu, H. Yoshida, M. Inayama, M. Yasumura and K. Taki, "Development of LVL frame structures using glued metal plate joints II: strength properties and failure behavior under lateral loading", *Journal of Wood Science*, vol. 46, pp. 193–201, 2000. https://doi.org/10.1007/BF00776449

[46] A. Özçifçi, "The effects of pilot hole, screw types and layer thickness on the withdrawal strength of screws in laminated veneer lumber", *Materials and Design*, vol. 30, pp. 2355–2358, 2009. https://doi.org/10.1016/j.matdes.2008.11.001

[47] G. Celebi and M. Kilic, "Nail and screw withdrawal strength of laminated veneer lumber made up hardwood and softwood layers", *Construction and Building Materials*, 21, pp. 894–900, 2007. https://doi.org/10.1016/j.conbuildmat.2005.12.015

[48] M. Dorn, K. Habrová, R. Koubek and E. Serrano, "Determination of coefficients of friction for laminated veneer lumber on steel under high pressure loads", *Friction*, 2020. https://doi.org/10.1007/s40544-020-0377-0

[49] C. Y. C. Purba, G. Pot, J. Viguier, J. Ruelle and L. Denaud, "The influence of veneer thickness and knot proportion on the mechanical properties of laminated veneer lumber (LVL) made from secondary quality hardwood", *European Journal of Wood and Wood Products*, vol. 77, pp. 393–404, 2019. https://doi.org/10.1007/s00107-019-01400-3

[50] P. Berard, P. Yang, H. Yamauchi, K. Umemura and S. Kawai, "Modeling of a cylindrical laminated veneer lumber I: mechanical properties of hinoki (*Chamaecyparis obtusa*) and the reliability of a nonlinear finite elements model of a four-point bending test", *Journal of Wood Science*, vol. 57, pp. 100–106, 2011. https://doi.org/10.1007/s10086-010-1150-1

[51] Y.-J. Song, S.-I. Hong, J.-S. Suh and S.-B. Park, "Strength performance evaluation of moment resistance for cylindrical-LVL column using GFRP reinforced wooden pin", *Wood Research*, vol. 62, no. 3, pp. 417–426, 2017.

[52] Z. Bednarek, D. Pieniak and P. Ogrodnik, "Wytrzymałość na zginanie i niezawodność kompozytu drewnianego LVL w warunkach podwyższonych temperatur", *Zeszyty Naukowe SGSP*, vol. 40, pp. 5–17, 2010. (in Polish)

[53] M. Bakalarz and P. Kossakowski, "The flexural capacity of laminated veneer lumber beams strengthened with AFRP and GFRP sheets", *Technical Transactions, Civil Engineering*, vol. 2, pp. 85–94, 2019. https://doi.org/10.4467/2353737XCT.19.023.10159

[54] M. Bakalarz and P. Kossakowski, "Mechanical properties of laminated veneer lumber beams strengthened with CFRP sheets", *Archives of Civil Engineering*, vol. 65, no. 2, pp. 57–66, 2019. https://doi.org/10.2478/ace-2019-0018

[55] M. Bakalarz, P. Kossakowski and P. Tworzewski, "Strengthening of bent LVL beams with near-surface mounted (NSM) FRP reinforcement", *Materials*, vol. 13, no. 10, article 2350, 2020. https://doi.org/10.3390/ma13102350

[56] B. Kawecki and J. Podgórski, "3D ABAQUS simulation of bent softwood elements", *Archives of Civil Engineering*, vol. 66 no. 3, pp. 323–337, 2020. https://doi.org/10.24425/ace.2020.134400

[57] B. P. Gilbert, H. Bailleres, H. Zhang and R. L. McGavin, "Strength modelling of Laminated Veneer Lumber (LVL) beams", *Construction and Building Materials*, vol. 149, pp. 763–777, 2017. https://doi.org/10.1016/j.conbuildmat.2017.05.153

[58] H. Valipour, N. Khorsandnia, K. Crews and S. Foster, "A simple strategy for constitutive modelling of timber", *Construction and Building Materials*, vol. 53, pp. 138–148, 2014. https://doi.org/10.1016/j.conbuildmat.2013.11.100

[59] N. Khorsandnia, H. R. Valipour and K. Crews, "Nonlinear finite element analysis of timber beams and joints using the layered approach and hypoelastic constitutive law", *Engineering Structures*, vol. 46, pp. 606–614, 2013. https://doi.org/10.1016/j.engstruct.2012.08.017

[60] M. Komorowski, "Manual of design and build in the STEICO system, Basic information, Building physics, Guidelines", Warsaw: Forestor Communication, 2017. (in Polish)

[61] European Committee for Standardization, EN 1990, Eurocode 0, Basis of structural design, European Committee for Standardization, Brussels, Belgium, 2002.

[62] European Committee for Standardization, EN 408, Timber structures - Structural timber and glued laminated timber - Determination of some physical and mechanical properties; European Committee for Standardization: Brussels, Belgium, 2012.

[63] European Committee for Standardization, EN 13183-1, Moisture content of a piece of sawn timber - Part 1: Determination by oven dry method; European Committee for Standardization: Brussels, Belgium, 2004.

[64] Abaqus 6.13 Documentation, Abaqus Analysis Users Guide, Abaqus Theory Guide.

[65] H. T. Nguyen and S. E. Kim, "Finite element modeling of push-out tests for large stud shear connectors", *Journal of Constructional Steel Research*, vol. 65, pp. 1909–1920, 2009. https://doi.org/10.1016/j.jcsr.2009.06.010

[66] M. P. Budziak and T. Garbowski, "Failure assessment of steel-concrete composite column under blast loading", *Engineering Transactions*, vol. 62, no. 1, pp. 61–84, 2014.

[67] M. Sciomenta, L. Spera, C. Bedon, V. Rinaldi, M. Fragiacomo and M. Romagnoli, "Mechanical characterization of novel homogeneous beech and hybrid beech-corsican pine thin cross-laminated timber panels", *Construction and Building Materials*, article 121589, 2020. https://doi.org/10.1016/j.conbuildmat.2020.121589

[68] Ł. Polus and M. Szumigała, "An experimental and numerical study of aluminium-concrete joints and composite beams", *Archives of Civil and Mechanical Engineering*, vol. 19, no. 2, pp. 375–390, 2019. https://doi.org/10.1016/j.acme.2018.11.007

[69] A. Pełka-Sawenko, T. Wróblewski and M. Szumigała, "Validation of computational models of steel-concrete composite beams", *Engineering Transactions*, vol. 64, no. 1, pp. 53–67, 2016.

[70] P. Szewczyk and M. Szumigała, "Welding deformation in a structure strengthened under load in an empirical-numerical study", in Advances in Mechanics: Theoretical, Computational and Interdisciplinary Issues. Proceedings of the 3rd Polish Congress of Mechanics (PCM) and 21st International Conference on Computer Methods in Mechanics (CMM), Gdansk, Poland, 8-11 September 2015, M. Kleiber, T. Burczynski, K. Wilde, J. Gorski, K. Winkelmann and L. Smakosz, Eds., London: CRC Press, 2016, pp. 563–566.

[71] P. Szewczyk, "Wzmacnianie pod obciążeniem belek zespolonych stalowo-betonowych w eksperymencie numerycznym i fizycznym", PhD thesis, West Pomeranian University of Technology in Szczecin, Poland, 2016. (in Polish)

[72] P. Różyło, "Stateczność i stany graniczne ściskanych cienkościennych profili kompozytowych", Lublin: Wydawnictwo Politechniki Lubelskiej, 2019. (in Polish)

[73] P. Rozylo, "Failure analysis of thin-walled composite structures using independent advanced damage models", *Composite Structures*, vol. 262, article 113598, 2021. https://doi.org/10.1016/j.compstruct.2021.113598

[74] A. B. Widodo, "Application of laminated veneer lumber (LVL) on the wooden boat construction", *IPTEK The Journal for Technology and Science*, vol. 23, no. 1, pp. 8–14, 2012.

Badania eksperymentalne i numeryczne paneli z drewna klejonego warstwowo z fornirów

Słowa kluczowe: drewno klejone warstwowo z fornirów, metoda elementów skończonych, wyroby drewniane, konstrukcje drewniane, konstrukcje zespolone, kryterium Hashin'a

Streszczenie:

W pracy przedstawiono wyniki badań zginanych paneli wykonanych z drewna klejonego warstwowo z fornirów (LVL). Materiał zgodny z ideą zrównoważonego budownictwa powstaje przez połączenie 3–4 mm fornirów za pomocą kleju. Autorzy badali zachowanie drewna klejonego warstwowo z fornirów, w którym wszystkie forniry są sklejone wzdłużnie – wzdłuż włókien (LVL R). Wyznaczono wytrzymałość materiału LVL R na rozciąganie, ściskanie

i zginanie. Określono zachowanie, nośność, formę zniszczenia paneli LVL R oraz zależność siła-przemieszczenie. Autorzy zaobserwowali formę zniszczenia paneli związaną z rozwarstwianiem warstw materiału oraz z pękaniem fornirów w rozciąganej strefie panelu. Przygotowano dwa modele numeryczne panelu LVL R i porównano ich zachowanie z laboratoryjną próbą zginania. W trójwymiarowym modelu numerycznym, zachowanie LVL R opisano za pomocą modelu sprężysto-idealnie plastycznego. W dwuwymiarowym modelu numerycznym materiał LVL R opisano, wykorzystując model ortotropowy a jego zniszczenie uwzględniono, biorąc po uwagę kryterium Hashin'a. Wyniki otrzymane z analiz numerycznych były zbliżone do rezultatów badań.